



**HAL**  
open science

## Energy and environmental performance of a new solar boiler with heat recovery for seawater desalination

Dylan Lorfing, Aras Ahmadi, Stéphanie Laborie, Régis Olives, Quentin Falcoz, Xavier Py, Ligia Tiruta-Barna

### ► To cite this version:

Dylan Lorfing, Aras Ahmadi, Stéphanie Laborie, Régis Olives, Quentin Falcoz, et al.. Energy and environmental performance of a new solar boiler with heat recovery for seawater desalination. Sustainable Production and Consumption, 2022, 32, pp.330-343. 10.1016/j.spc.2022.05.001 . hal-03692778

**HAL Id: hal-03692778**

**<https://hal.science/hal-03692778>**

Submitted on 10 Jun 2022

**HAL** is a multi-disciplinary open access archive for the deposit and dissemination of scientific research documents, whether they are published or not. The documents may come from teaching and research institutions in France or abroad, or from public or private research centers.

L'archive ouverte pluridisciplinaire **HAL**, est destinée au dépôt et à la diffusion de documents scientifiques de niveau recherche, publiés ou non, émanant des établissements d'enseignement et de recherche français ou étrangers, des laboratoires publics ou privés.

# Energy and environmental performance of a new solar boiler with heat recovery for seawater desalination

Dylan Lorfing <sup>a</sup>, Aras Ahmadi <sup>a</sup>, Stéphanie Laborie <sup>a</sup>, Régis Olives <sup>b</sup>, Quentin Falcoz <sup>b</sup>,  
Xavier Py <sup>b</sup>, Ligia Tiruta-Barna <sup>a</sup>

<sup>a</sup> TBI, Université de Toulouse, CNRS, INRAE, INSA, Toulouse,, France

<sup>b</sup> PROMES-CNRS, Université de Perpignan Via Domitia, Tecnosud, Rambla de la Thermodynamique, 66100 Perpignan, France

## Highlights

- A novel beam-down concentrated solar power boiler is developed.
- The “from sea and sun to tap water” installation is modeled.
- Greenhouse gas emission is 86% less than that of conventional thermal desalination.
- A 61% reduction in power consumption is achieved compared with reverse osmosis.

## Abstract

This study proposes a new seawater desalination process using concentrated solar energy. Compared with conventional desalination technologies, the proposed process produces tap water with high energy efficiency and a lower environmental impact.

The proposed process is based on a new type of solar boiler using solar energy concentrated via a “beam-down” optical system. To improve the productivity, the steam produced is used to feed an adapted multiple-effect distillation (MED) system. A complete process model from seawater and sun to tap water is proposed, coupling an in-house Python program for the solar boiler component and ProSim software for the MED component. Ancillary calculations concerning the pretreatment, post-treatment, and sizing of the components are performed using a spreadsheet program. The environmental impacts of the tap water production by the proposed system are evaluated using the life cycle assessment method.

The theoretical feasibility of the proposed process is demonstrated by modeling a reference case, with an estimated annual productivity of 10,000 m<sup>3</sup> of tap water. According to the calculation, the energy performance is estimated at 1.57 kWh of electricity and 117.7 kWh of solar energy per cubic meter of tap water produced. An estimated land area of 3,845 m<sup>2</sup> is required for the solar field. The life cycle assessment indicates that the performance of the proposed process is significantly improved compared with conventional MED, with an 84% reduction in the total impact according to the ReCiPe endpoint method. In addition, the proposed system displays a competitive environmental performance compared with reverse osmosis. The emissions of the new process are estimated at 2.36 kg CO<sub>2</sub>-eq per cubic meter of tap water produced versus 3.67 kg CO<sub>2</sub>-eq and 2.97 kg CO<sub>2</sub>-eq for low- and high-performance reverse osmosis, respectively.

Keywords: Solar desalination, concentrated solar energy, life cycle assessment, process modeling, process ecodesign

## Nomenclature

<i>CSP</i>	Concentrated Solar Power
<i>DNI</i>	Direct Normal Irradiance [ $\text{W m}^{-2}$ ]
<i>GOR</i>	Gain Output Ratio
$\dot{m}$	Mass Flow Rate [ $\text{kg s}^{-1}$ ]
<i>MED</i>	Multiple-Effect Distillation
<i>P</i>	Pressure [Pa]
<i>PV</i>	Photovoltaic
$\dot{Q}$	Power [W]
<i>RO</i>	Reverse Osmosis (without energy recovery)
<i>ROR</i>	Reverse Osmosis (with energy recovery)
<i>S</i>	Surface [ $\text{m}^2$ ]
<i>s</i>	Salinity [ $\text{kg}_{\text{NaCl}} \text{kg}^{-1}$ ]
<i>SB</i>	Solar Boiler
<i>SB-MED</i>	Solar Boiler-Multiple-Effect Distillation
<i>T</i>	Temperature [K]
Greek symbols	
$\eta$	Efficiency

### *Sub/superscripts*

<i>bd</i>	Beam-Down
Boiling	Transfer by Film Boiling
brine	Brine
$\text{H}_2\text{O}$	Water
loss	Losses by Receiver Upper Side
NaCl	Sodium Chloride Salt
Solar	Concentrated at Receiver Level
steam	Steam
sw	Seawater
wall	Losses by Solar Boiler Tank Wall

## 1 Introduction

The growing world population, combined with increases in per capita water consumption, has led to an over-exploitation of natural freshwater resources [1]. Several geographical areas are already facing freshwater shortages, and climate change could worsen the situation [2],[3]. Because salt water represents 97.5% [4] of all water on Earth, desalination is one possible response to freshwater scarcity. Desalination has been used for decades, and several countries currently depend on it for their water supply [5],[6]. Of the proposed technologies, the most widely used at the industrial level are reverse osmosis (RO) and multiple-effect distillation (MED). The first uses semipermeable RO membranes to separate a pressurized flow of seawater into two flows: permeate and brine [7]. The second, MED, is composed of a succession of “effects” in which the condensation of the steam of the previous effect enables the vaporization of seawater [8]. Usually, the feeding steam of the first effect is provided by a boiler powered by fossil fuels. One of the major acknowledged drawbacks of desalination processes, such as classical distillation, multi-stage flash distillation, and MED, is their intensive consumption of heat energy [9]. Despite the considerable progress achieved in this field, following significant research effort and years of feedback, the energy consumption of desalination remains high and is responsible for significant environmental impacts [10].

Energy transitions linked to the growing needs of water consumption require innovative solutions. There is a great diversity of solutions proposed to alleviate this energy issue, from the use of geothermal energy to provide heat for thermal desalination processes to the use of wind or tidal energy to supply power to RO installations [11]-[13]. Of the proposed solutions, solar energy has received considerable attention [6],[14]. Indeed, solar energy is one of the most explored renewable resources, in particular because there is a strong correlation between areas with high solar potential and areas where freshwater shortages are most significant [15]. These points make solar energy particularly interesting in the context of desalination.

Of the various solutions, the coupling of photovoltaic (PV) electricity production with RO systems has already been extensively studied [16],[17]. Another promising solution is the use of waste heat from concentrated solar power (CSP) plants to feed a thermal desalination system, e.g., MED. Solar stills have also been studied, primarily for small-scale installations, because of their ease of use and their potential in remote areas [18],[19]. Despite the diversity of the proposed solutions, only a few large-scale solar desalination projects have been implemented or even planned.

The alternative solutions that have already been considered are promising but suffer from several limitations. Regarding PV-RO systems, the performance of the entire system is limited by the PV performance. CSP-MED systems appear to have significant potential; however, electricity production is not always required at a given site and increases the complexity of the system. The use of many loops with different fluids requires a large number of heat exchangers between the loops to ensure heat transfer. This complexity is particularly limiting for small-scale applications. Finally, the efficiency of solar stills remains limited and implies the use of a large land area [6].

To overcome these difficulties, a new conceptual process for seawater desalination using solar energy as the main energy source is proposed in this study. The proposed process is based on a newly developed solar boiler [20]. The solar boiler permits seawater to be distilled using solar energy concentrated via a “beam-down” optical system. The beam-down system consists of a two-reflection device, which allows the concentration of solar energy at the ground level in a downward-directed beam [21]. This system, initially developed for CSP applications, presents several advantages for use in various applications other than power generation [22]: (i) the vertical downward concentration and the radiation focused at the ground level facilitate energy use for various processes; (ii) the point

concentration allows work over a wide temperature range; and (iii) the construction costs are less than those of conventional solar towers. In this study, the steam produced by the solar boiler (SB) is used as the input stream in the first stage of an adjusted MED system in order to improve the energy efficiency and water productivity.

A comprehensive model coupling the SB with MED (SB-MED) is developed here, complete with all the ancillary processes required for tap water production, from seawater pumping to tap water delivery. The objective of the modelling is to evaluate the entire process in terms of the technical, energetic, and environmental performances. The model considers the particularities of the newly proposed SB (i.e., its shape and material) and the main characteristics of the beam-down solar installation (the reflection surface and optical efficiency). The MED is simulated by rigorously integrating the mass and heat balances, as well as the thermodynamics, for the non-ideal behavior of seawater. The model is applied to a theoretical reference case, a small desalination installation producing drinking water for a small community, with a target annual productivity of 10,000 m<sup>3</sup> of tap water. The environmental performance is assessed using the life cycle assessment (LCA) method [23] to identify the hot spots of the system and to ultimately compare the new system with conventional technologies. The comparison of the technical, energetic, and environmental performances of SB-MED enables this system to be placed in the context of other desalination systems and highlights its strengths and limitations. To the best of the author's knowledge, this is the first study proposing such solar based desalination technology and its detailed modeling and performance assessment.

## 2 Materials and Methods

### 2.1 Description of a new process coupling concentrated solar boiling with heat recovery via multiple-effect distillation (SB-MED)

The complete process of tap water production from seawater, shown in Figure 1, is based on a newly developed SB that enables the production of steam from seawater using concentrated solar energy provided by a beam-down system. The steam is condensed to produce distilled water. The condensation heat extracted from the steam is then used as a heat source in a thermal desalination process based on MED. Pumping, pretreatments, and post-treatments, also represented on Figure 1, are considered and are based on conventional treatments currently used in thermal desalination processes; these steps are detailed in Section 2.2.4 [24].

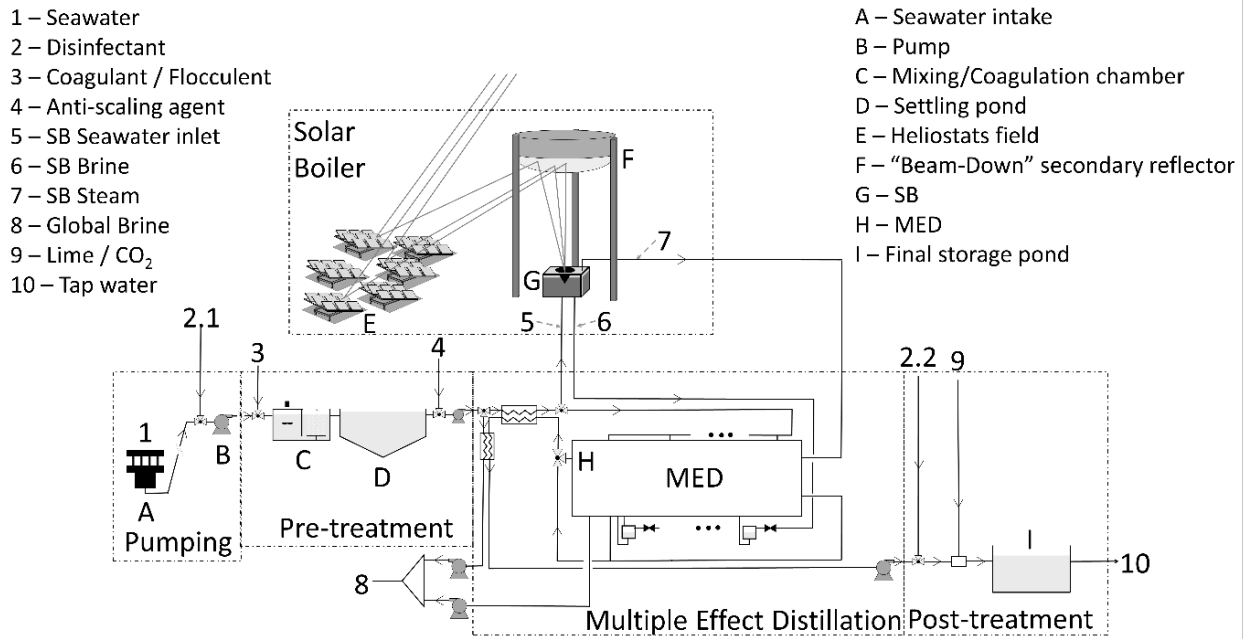


Figure 1: Layout of the solar boiler (SB)-multiple-effect distillation (MED) system.

The solar boiler (SB)

The central element of the proposed process is the SB, which is composed of three parts.

First, a solar collector concentrates solar energy in a downward vertical flow. The concentrator is based on the beam-down concept, shown in Figure 2A. The beam-down apparatus consists of a field of heliostats (Figure 2A-1) that reflect the solar direct normal irradiation (*DNI*) at the top of a structure supporting a secondary reflector (Figure 2A-2). The secondary reflector redirects the collected solar energy toward the ground to the focal point (Figure 2A-3).

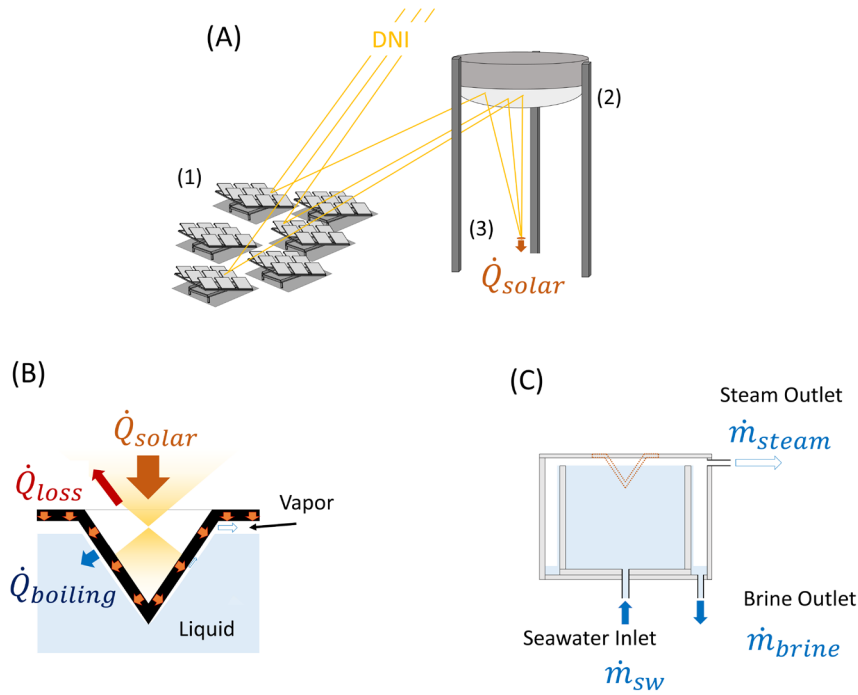


Figure 2: Illustration of the SB showing (A) the beam-down concentrator, (B) the receiver, and (C) the tank.

The second element is the conical receiver installed at the focal point. This receiver converts the useful part of the radiative power ( $\dot{Q}_{solar}$ ) into heat and then transfers it to the seawater via boiling ( $\dot{Q}_{boiling}$ ). The power that is not transmitted to the seawater ( $\dot{Q}_{loss}$ ) is lost to reflection, radiation, and convection. The conical receiver and the heat transfer flux are represented in Figure 2B. The SB is especially designed to operate under film-boiling conditions. This choice was motivated by the protective effect on the receiver of the vapor film between the receiver and the seawater, which prevents salt crusting.

Finally, the third part of the SB is the tank, shown in Figure 2C. The tank is supplied with seawater at a given flow rate ( $\dot{m}_{sw}$ ). A first outlet at the top of the tank allows the recovery of the produced vapor at a flow rate of  $\dot{m}_{steam}$ . A second outlet at the bottom of the tank allows the brine, at a flow rate of  $\dot{m}_{brine}$ , to be evacuated. Details concerning the modeling and design of the SB are given in Section 2.2.2.

### The adapted multiple-effect distillation (MED)

Vapor and brine produced by the SB are routed to an MED whose characteristics have been adjusted (Figure 3B) while keeping its essentials similar to those of conventional installations (Figure 3A) [8]. As in conventional installations, the adapted MED is constructed of a succession of stages. Each stage consists of a vessel making use of the principle of evaporation and condensation at a reduced ambient pressure. On the hot side of each vessel, inlet steam from the SB or the previous effect is condensed. On the cold side, seawater inlet at a reduced pressure is partially vaporized. The evaporation takes place on the surfaces of the hot heat transfer tubes on which the seawater is sprayed.

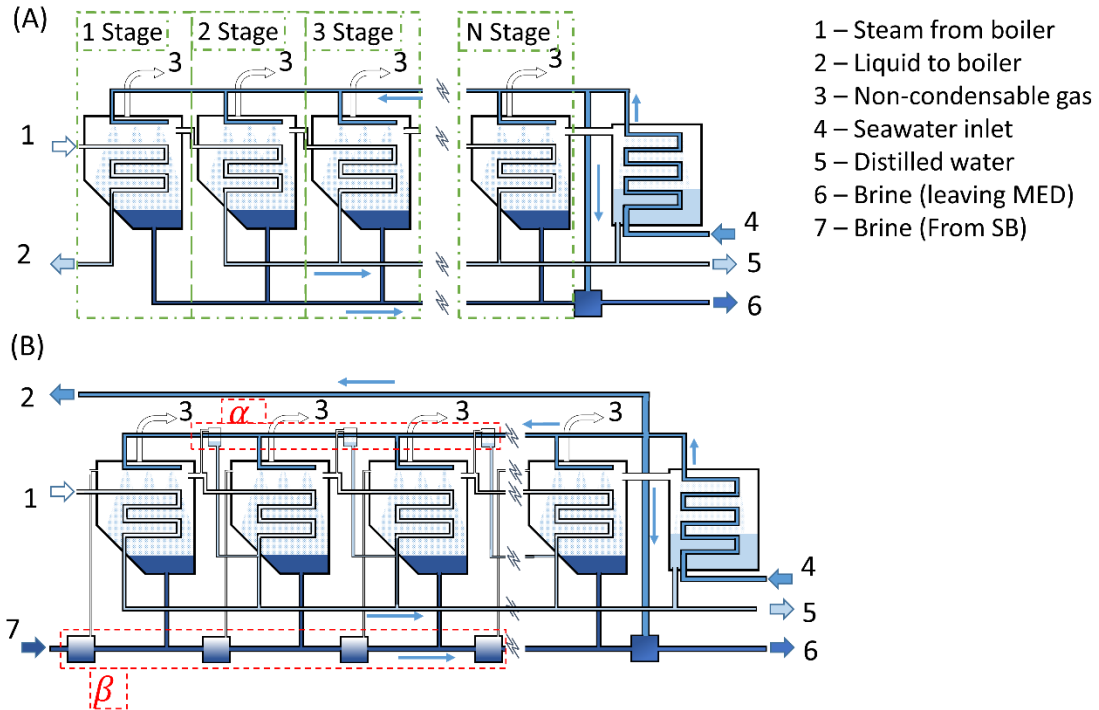


Figure 3: Layout of (A) a conventional MED system and (B) one upgraded and adapted for operation with the SB.  $\alpha$ : seawater preheating;  $\beta$ : flash chambers

The steam produced at one stage is condensed in the next stage inside the heat transfer tubes and then collected.

Many improvements to increase the performance of conventional MED systems have been proposed in the literature and are used in industry. In the present study, two classical upgrades are considered. The first is seawater preheating (Figure 3B- $\alpha$ ). At each stage, a fraction of the produced vapor is extracted and its condensation heat is used to preheat the entering seawater. The second upgrade consists of installing a flash chamber between each stage at the corresponding pressure (Figure 3B- $\beta$ ). Brine extracted from the different stages is sent to the flash chamber, permitting the extraction of a small portion of vapor that can be used to complement the incoming steam.

In the final stage, steam condensation is ensured in a condenser by an additional flow of seawater. The seawater used for cooling is then mixed with the brine and discharged into the sea. This mixing permits the salt concentration of the brine to be reduced prior to discharge, reducing its impact on the environment. The temperature and pressure levels, design parameters of the MED, and adaptations made to couple it with the SB are presented in detail in Section 2.2.3.

## 2.2 Process modeling and technical and energetic performances of the SB-MED process

### 2.2.1. Main steps of the modeling approach

The key processes involved in the proposed desalination system are the SB and the MED, which require specific models based on the mass and energy balance and their design and sizing. The SB model was developed and evaluated using an in-house-developed Python program. The simulation of the MED was performed using the state-of-the-art ProSim<sup>®</sup> chemical engineering simulation software. The pre- and post-treatment processes are not new; they are well-described by conventional models with respect to their material and energy balances and their design. The energy

and chemical consumptions of the pre- and post-treatment processes were calculated on an Excel spreadsheet. Details concerning the parameters needed for these estimations are based on the literature and are briefly summarized in Appendix 1.

The global structure of the modeling approach and the tools used for the calculation and simulation are presented in Figure 4.

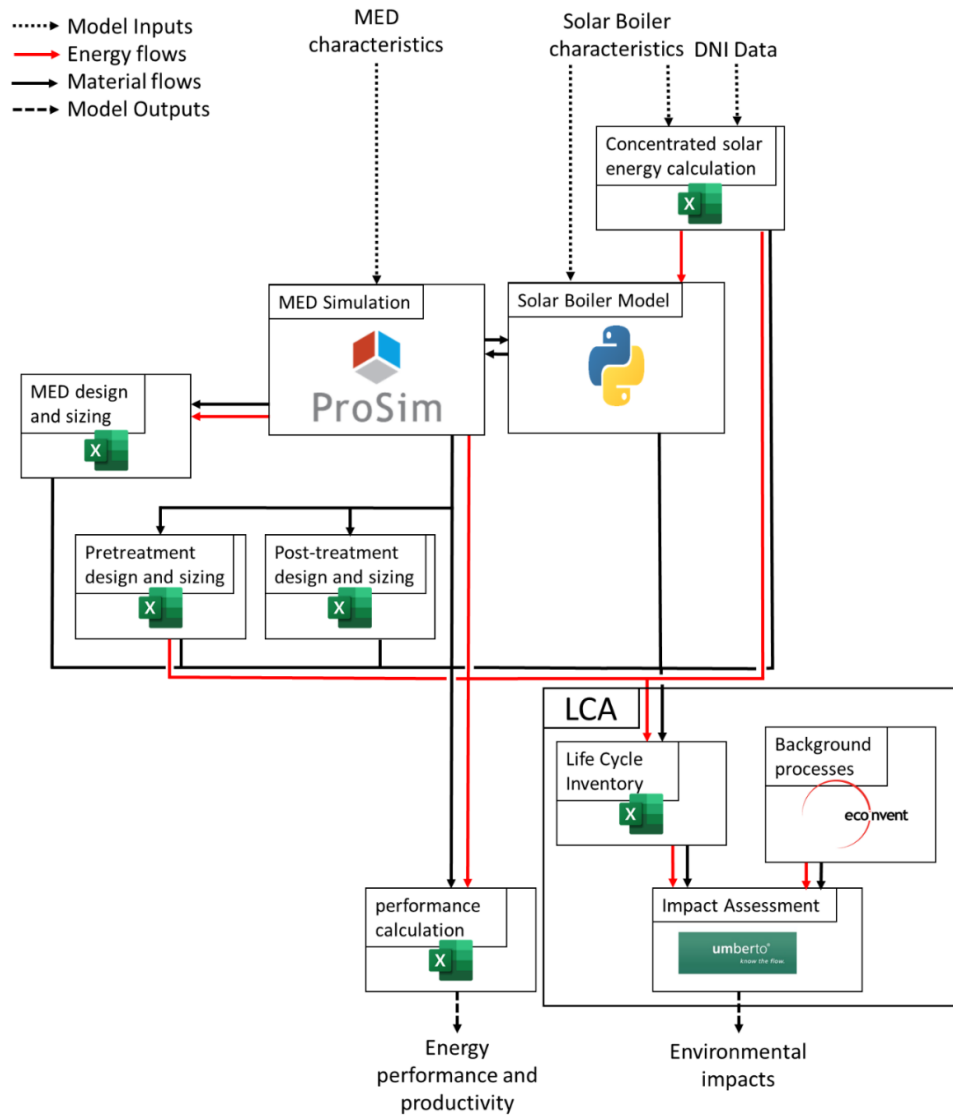


Figure 4: Architecture of the modeling approach for the SB-MED system and for the energy, productivity, and environmental performance calculations.

The material inventory required for the construction of the system and estimations of the concentrated solar power and the annual operation hours were all made in Excel. Finally, the environmental impacts were calculated using the LCA Umberto<sup>®</sup> software [25], with the foreground inventory provided by the modeling platform and with the background inventory supplied by the ecoinvent database (Section 2.3) [26].

### 2.2.2 SB and solar concentrator

To estimate the productivity of the process under realistic conditions, a small-scale reference case is proposed and studied here. The reference case is designed for a desalination unit on the

Mediterranean island of Corsica. The production goal of the reference installation was set to 10,000 m<sup>3</sup> of tap water per year. A conventional reference *DNI* value of 1,000 W m<sup>-2</sup> was assumed given the sizing. Based on the usual local solar resources [27], the operating hours of the installation were then estimated at 1,885 h yr<sup>-1</sup>.

The dimensions of the beam-down system used are based on those of a 100-kW laboratory-scale installation [21]. The dimensions of the heliostat field therefore needed to be adjusted to provide the necessary energy to achieve the production goal.

Losses occur during the collection of solar energy. To take this into account and to estimate the power concentrated by the beam-down system, Equation (1) is used:

$$\dot{Q}_{solar} = \eta_{bd} S_{collec} DNI, \quad (1)$$

where  $\dot{Q}_{solar}$  is the power concentrated at the receiver [W], *DNI* is the direct normal irradiation [W m<sup>-2</sup>], *S<sub>collec</sub>* is the total surface of the primary mirrors [m<sup>2</sup>], and  $\eta_{bd}$  is the optical efficiency of the beam-down installation, accounting for the different losses during the collection and concentration of the solar energy. These losses are due to the cosine effect, reflectivity, blocking effect, shadow effect, and aim error. The combination of these losses (or efficiencies, as presented in Table 1) indicates an estimated global optical beam-down efficiency,  $\eta_{bd}$ , of 0.58. Note that the optical efficiency of the installation depends on the position of the Sun. Here, only the annual mean values are presented. These values are used in this study as a first approximation.

Table 1: Various estimated efficiency factors [28].

Efficiency	Reflectivity	Cosine effect	Blocking and shadow effect	Aim error
Value	0.85	0.90	0.95	0.97

The method proposed by Lorfing et al. [20] was used to model the receiver and the tank of the concentrated SB. Concerning the modeling of the concentrated SB, the following energy balance equation is considered around the receiver:

$$\dot{Q}_{solar} + \dot{Q}_{loss} + \dot{Q}_{boiling} = 0, \quad (2)$$

where  $\dot{Q}_{solar}$  is the concentrated solar energy reaching the receiver,  $\dot{Q}_{loss}$  represents the heat losses resulting from radiation, convection, and reflection on the upper side of the receiver [W], and  $\dot{Q}_{boiling}$  is the heat transmitted to the boiling fluid at the lower side of the receiver. These flows are represented in Figure 2B. Then, the following heat and mass balance equations can be written for the fluid in the SB tank.

$$\dot{m}_{sw,H_2O} = \dot{m}_{steam,H_2O} + \dot{m}_{brine,H_2O} \quad (3)$$

$$\dot{m}_{sw,NaCl} = \dot{m}_{brine,NaCl} \quad (4)$$

$$\dot{m}_{steam}(h_{steam} - h_{in}) + \dot{m}_{brine}(h_{brine} - h_{in}) + \dot{Q}_{boiling} - \dot{Q}_{wall} = 0 \quad (5)$$

In Equation (4), the mass flow of salt leaving the SB is obtained by assuming that the vapor formed by boiling is pure water.

A nodal method is considered for the resolution. This method considers the temperature at the upper and lower surfaces of the receiver, the boiling temperature of the seawater in the SB, the temperature of the entering seawater, and the ambient temperature.

The liquid–vapor equilibrium condition allows the boiling temperature to be related to the operating pressure in the SB.

$$P = P_{sw}^{sat,*}(T_b, s) \quad (6)$$

To complete the model, equations for each heat transfer phenomenon are included using expressions from the literature. The radiative and reflective losses are expressed following the method proposed by Modest [29] for a grey surface at a constant temperature. Conduction through a plate is considered for the heat transfer between the upper and lower surfaces of the receiver. The convective phenomena are described via equations for natural convection over a flat plate (for the horizontal part of the receiver) and an inclined plate (for the conical part). These equations are taken from Rohsenow et al. [30]. Free convection is considered in the same manner for the heat lost by the tank. Finally, the heat transfer between the receiver and the boiling fluid is treated as the heat exchange via boiling under film conditions, with equations taken from [30]. The CoolProp library [31] was employed to calculate the fluid properties and the phase equilibrium conditions in the SB.

The SB model makes it possible to determine the energy efficiency and productivity of the SB depending on the operating conditions ( $\dot{Q}_{solar}$ , flow rates, fluid specificity, temperature, and pressure) and the SB design and sizing parameters (e.g., system geometry and material properties).

In the reference case, the geometric parameters of the SB receiver were chosen to maximize the vapor production at the operating point ( $DNI = 1,000 \text{ W m}^{-2}$ ). Its dimensions were also chosen to maintain a sufficiently high temperature at the lower surface to maintain the film-boiling regime for a  $DNI$  as low as  $500 \text{ W m}^{-2}$ .

The power input was chosen to ensure the necessary steam production to reach the annual production goal. Because the SB is designed to work with seawater, boiling was assumed at atmospheric pressure at a vaporization rate of 0.65. All the operating conditions used for the calculations are summarized in Table 2.

Table 2: Operation conditions at the inlet for the simulation of the solar boiler (SB)-multiple-effect distillation (MED) system.

Principal characteristics of the SB-MED calculation		
SB		
Operating pressure	101,325	Pa
Vaporization rate	0.65	
MED		
Number of stages	14	
Top-stage temperature	70	°C
Last-stage temperature	35	°C
Temperature change ( $\Delta T$ ) between each stage	2.5	°C
Maximal discharge temperature	$T_{sw} + 10$	°C
Total distillate water flow	5,303	kg h <sup>-1</sup>
Inlet seawater		
Salinity	0.039	kg <sub>NaCl</sub> kg <sub>sw</sub> <sup>-1</sup>
Temperature	20	°C

### 2.2.3 Simulation and performance of the adjusted MED system

As mentioned in Section 2.2.1, the adjusted MED system was simulated using the state-of-the-art ProSim<sup>®</sup> chemical engineering simulation software.

In this approach, the seawater is treated as a binary mixture of water and sodium chloride. To account for the discrepancy between an ideal fluid and the seawater (an electrolyte solution), a heterogeneous approach was applied. The activity coefficients were estimated by the e-NRTL model, and the fugacity of pure water was calculated via the Henry law, with the Poynting correction. The Peng–Robinson equation of state was used for the water gas phase.

As mentioned in the process description (Section 2.1), the adjusted MED is based on a conventional MED with preheating of the incoming seawater and flashing of the brine, as can be seen in the layout of the installation (Figure 3B). The number of effects usually varies between 4 and 21 [32]; in this case, 14 stages were considered, with a top temperature of 70°C. This temperature corresponds to the usual temperature at the top of an MED necessary to avoid corrosion [24]. The temperature at the last stage was set to 35°C. This value is also usual for an MED system and permits the boiling to occur at a reasonable pressure level. The seawater inlet was set to 20°C at atmospheric pressure. The pressure level was calculated for each stage to ensure a temperature difference between the condensation temperature of the steam and the boiling temperature of seawater of 2.5°C, which is necessary for the heat transfer.

The distillate flow rate target at the operating point was set to 5,303 kg h<sup>-1</sup>. This rate was fixed according to the annual production goal (10,000 m<sup>3</sup>) and the number of expected operating hours (1,885 h). The seawater flow rate entering the SB-MED was then determined to ensure the target flow. In this study, the seawater flow was equally spread between the SB and each stage of the MED.

The cooling seawater flow necessary for the final condensation and to cool the distilled water enters the system at 20°C. After its use and before being rejected to the sea, the cooling water is mixed with the brine, lowering the salt concentration of the discharge and decreasing its potential impact on the environment. The flow rate of the cooling seawater was determined to ensure a maximal temperature difference of 10°C between the discharge and the seawater.

The design was adapted to couple the MED with the SB. The vapor coming from the SB is condensed in the first stage of the MED, allowing vaporization of the seawater in this stage. Contrary to a conventional installation, the condensate vapor from the SB is collected with all of the other condensates from the MED and is part of the final distillate production. The brine coming from the SB is collected, as is the other brines from the MED, and sent to the flash chamber to increase the vapor production.

The electricity consumption used for pumping was estimated based on the mass flow and the required pressure drops, with a pump efficiency and an electric motor efficiency of 0.70 and 0.98, respectively [33]. The incondensable gas mass flow that needs to be evacuated to maintain the necessary low pressure was assumed to represent 0.06% of the vaporized seawater mass [34].

The parameters necessary for the MED simulation are summarized in Table 2.

### 2.2.4 Pumping, pretreatment, and post-treatment

The first step in the process is seawater pumping to the facility. Based on current practical operations, it is assumed that the distance between the installation and the seawater intake is equal

to 3,500 m. The pressure drop for seawater transport is estimated to be 3.2 bar [35]. The electricity consumption for the pumps is estimated as presented in the previous section. At the seawater intake (Figure 1A), a large mesh filter prevents the intake of large particles and disinfection with hypochlorite prevents the growth of algae or microorganisms (Figure 1-2.1).

To ensure the proper operation of the equipment, the seawater needs to be pretreated before being used in the SB-MED process. The pretreatment consists of adding a coagulant and a flocculant (Figure 1-3) in a mixing and flocculation tank (Figure 1-C). Next, sedimentation is performed in a suitable pond (Figure 1-D). Finally, an antiscalant is added to the seawater (Figure 1-4). The chemicals used for these treatments and their required quantities, the size of the necessary equipment, and the associated electricity consumption are estimated using data and methods given in the literature [36].

The distilled water obtained at the outlet of the SB-MED system is remineralized in a post-treatment step using lime (Figure 1-9), and then a disinfection step is performed to avoid any contamination (Figure 1-2.2). As for the pretreatment, the type and size of the required equipment were estimated according to conventional methods found in the literature; details are given in Appendix 1.

## 2.3 LCA of the SB-MED system and comparison with conventional desalination technologies

The data, assumptions, and equations presented in Sections 2.1 and 2.2 allow an estimation of the technical performance and energy (electricity) consumption of the proposed system for a given annual production goal, i.e.,  $10,000 \text{ m}^3 \text{ yr}^{-1}$ . Based on the calculated performances, the proposed process can be compared with more conventional desalination technologies for the same level of tap water production. The three selected comparative scenarios are presented in Section 2.3.1. The particularities of SB-MED are its use of concentrated solar energy as the main energy source in the SB and its corresponding adjustment of the MED system to maintain a reasonable rate of desalination. For these reasons, a comparison based only on the energy performance cannot fully demonstrate the appeal of the presented process. To obtain a better understanding of the strengths and limitations of the scenario, a full LCA of the SB-MED system needs to be presented with the analysis of the energy performance.

### 2.3.1 Comparative scenarios

The three conventional desalination scenarios that are compared with SB-MED are (1) a conventional MED using the combustion of natural gas to supply heat; (2) a conventional one-pass RO desalination system; and (3) a one-pass RO system with an integrated turbine to recover energy from the brine under pressure (referred to here as ROR).

#### Conventional MED

The conventional MED process follows a more or less similar design to that of the MED part of the SB-MED process; see the layout in Figure 3B. The main difference is that the gas boiler of the conventional system is supplied with pure water in a closed loop, where the operating conditions are correspondingly defined to be compatible with the same scale of production as selected for the SB-MED process (see 3.1). Therefore, unlike in the case with the SB, the steam from the hot side of the first evaporator is returned to the boiler and is not extracted with the rest of the distilled water.

The conventional MED process was simulated using the ProSim software. The gas boiler steam flow and the seawater inlet flow were chosen to achieve the same annual productivity of tap water as that with the SB-MED process. Accordingly, the proposed MED was designed and sized to produce  $10,000 \text{ m}^3$  of tap water per year. Because the conventional MED operates with fossil fuel, two stops of 48 h per year were included for maintenance, resulting in an estimate of the necessary distillate

flow of  $1,154 \text{ kg h}^{-1}$  for this scenario. Details concerning the MED characteristics are given in Appendix 2.

#### RO without energy recovery

The considered RO system is illustrated in Figure 5-RO. It is composed of a pump that pressurizes the seawater and the RO modules, which split the seawater into two flows, i.e., into demineralized water and brine. The demineralized water is sent to post-treatment, as described for the distilled water in the SB-MED process, and the brine is sent back to the sea. The pressure level depends on the number of modules, their organization (in series and/or in parallel), their characteristics, the production objective, and the recovery rate. The annual production objective was set to  $10,000 \text{ m}^3$  of tap water.

To determine the number of modules and the required pressure levels, the CSMPRO 6 commercial software was used [37]. This software allows the characteristics of commercial modules to be considered. The global recovery rate was set to 42.5%.

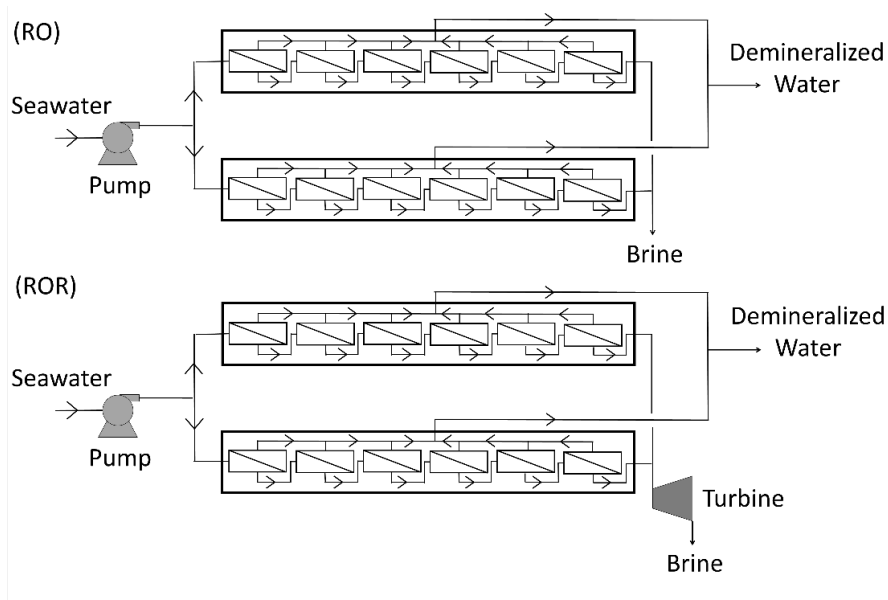


Figure 5: Layout of the reverse osmosis facilities in the cases of RO (without energy recovery; top) and ROR (with energy recovery; bottom).

The energy demand necessary for the pressurizing seawater was calculated assuming the same efficiency for the pump as in the SB-MED process. In addition, compared with the SB-MED process, the necessary pretreatments are more important in the RO installation to guarantee the performance of the installation before performing RO. Details concerning the process modeling and pretreatment are given in Appendix 2.

#### RO with energy recovery (ROR)

To reduce the energy demands of RO systems, recent industrial facilities use recovery devices to recapture part of the energy from the brine under pressure. To provide a fair energy-wise comparison, this scenario was also considered in our study. The installation of an ROR system is similar to that of the RO system; however, a turbine is added to the brine outlet to generate electricity (Figure 5-ROR). The produced electricity compensates for part of the electricity consumption needed for the seawater pressurization. The production of electricity can be estimated

from the brine and pressure flow rates. The efficiencies of the turbine and generator energy conversions were taken from the literature.

### 2.3.2 LCA: Goal and scope

In the following, the LCA application to the desalination system is described according to the four steps of the methodology: (1) defining the goal and scope of the LCA study, (2) building an inventory of all the materials and energy flows, (3) calculating the associated impacts using life cycle impact methods, and (4) interpreting the results and making recommendations for improvements.

In this study, the objective of the LCA is to evaluate the potential performance gain, from an environmental point of view, of the proposed SB-MED process with respect to conventional desalination processes. LCA is applied to the reference case presented in Section 2.2 for the proposed process, as well as the three conventional desalination processes presented in Section 2.3.1. The functional unit is the production of 1 m<sup>3</sup> of tap water by a small-scale desalination system over a period of 40 years on a Mediterranean island (Corsica). The production capacity is 10,000 m<sup>3</sup> of tap water per year. A cradle-to-gate boundary is adopted, considering all processes from raw resource extraction to the final product, i.e., tap water. The foreground system encompasses the entire process from seawater pumping to storing the tap water in a tank ready for use. LCA was performed using the Umberto software and the ecoinvent 3.7 database, employing the default allocation model (APOS).

### 2.3.3 Life cycle inventory

The inventory for the foreground process includes the material and energy consumption for the desalination process operation from seawater to the final tap water, as well as materials used for the equipment and infrastructure.

The material and energy consumptions for the process operation were calculated based on the modeling approaches described in Section 2.2 for the SB-MED process and in Section 2.3.1 for the three conventional processes, with related information concerning the referenced literature and other details given in Appendices 1 and 2.

Except for the beam-down system associated with the SB-MED scenario, it was assumed that all items were placed inside a building, the construction of which needs to be considered. The materials used for construction, the equipment, and the space required for the SB were estimated based on recommendations and data from the literature [21],[38] and on the models presented in Sections 2.2 and 2.3.1 and in Appendices 1 and 2.

The inventory for the background processes (e.g., material and chemical production, energy production, transportation, and waste treatment) were taken from the ecoinvent database [26]. Regarding the electricity used, the reference mix was set to the Italian electricity mix because of its similarity with the Corsican mix (not present in the database). The process system for LCA, namely the background and foreground processes and their connections and exchanges with the environment, is illustrated in Figure 6 for the SB-MED scenario.

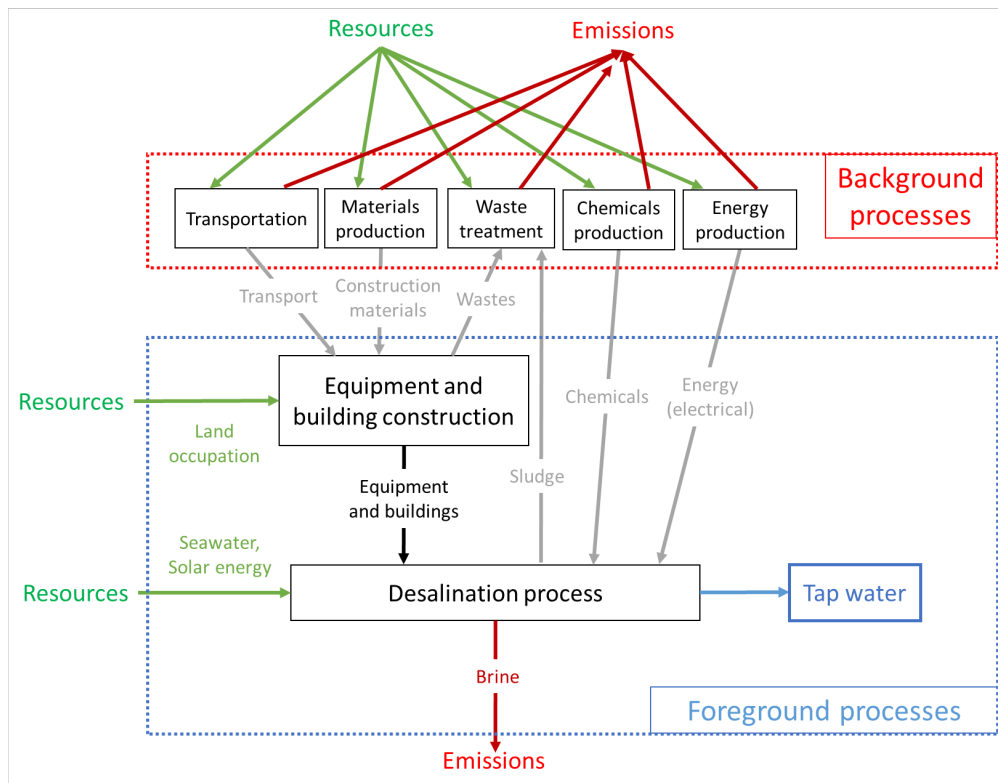


Figure 6: Life cycle assessment (LCA) process system diagram for the SB-MED scenario.

### 2.3.4 Life cycle impact assessment

The environmental impacts were calculated using the ReCiPe method with the endpoint indicators. This method calculates 17 categories of endpoint impacts, assessing the damages with respect to three areas of protection, i.e., ecosystem quality, human health, and resource depletion. In addition, because it is a major issue of topical interest, the climate change impact was calculated using the IPCC 2013 method.

## 3 Results and Discussion

### 3.1 Calculated productivity and characteristics of the SB-MED system in comparison with standalone SB

An annual production of 10,000 m<sup>3</sup> of tap water (5,303 kg h<sup>-1</sup>) with a solar resource of 1,885 kWh m<sup>-2</sup> yr<sup>-1</sup> is considered, corresponding to the demands of 228 persons, assuming a consumption of 120 L day<sup>-1</sup> per capita.

The coupled SB-MED model, associated with the input parameters (the available solar energy resources and the required tap water production) and all hypotheses presented in Section 2, allows estimations of the heat and material flows for the entire desalination process, as well as the capacity of the required installations (i.e., the beam-down system, SB, and MED).

#### 3.1.1. Size and potential optimization of the solar field

Concerning the beam-down system, to ensure the production required for the reference case, 363,414 W of energy needs to be concentrated at the focal point when the *DNI* is equal to 1,000 W m<sup>-2</sup>. These figures combined with Equation (1) allow an estimation of the required dimensions of the solar concentrator needed to achieve the production goal. The principal characteristics of the beam-down system calculated for this reference case are given in Table 3. For the reference case, the first reflection surface needs to have an area of 625 m<sup>2</sup> and the height of the reflector tower needs to be equal to 20 m. These dimensions appear to be realistic for a small-scale installation. Indeed, these characteristics are slightly larger than those of the experimental beam-down system presented in the literature [21],[39] but smaller than those mentioned in existing industrial projects [40],[41]. Note, however, that the heliostat field geometry is not optimized. Moreover, the mean reflectivity considered for the mirrors is very conservative and it is reasonable to consider that an optimized concentrator with a high-performant and well-maintained material could result in a significant reduction in the concentrator size for the same final concentrated power.

### 3.1.2 Dimension and materials selected for the solar boiler

As explained in Section 2, the SB is the main novel feature of the proposed system. The retained geometric characteristics are presented in Table 3. With this geometry, the model resolution (presented in Section 2.2.2) permits an estimate of the mean expected receiver temperature of approximately 520°C, with a corresponding surface heat transfer of 9.6 W cm<sup>-2</sup>. This high temperature required for film-boiling operation is expected to allow seawater boiling in the SB at atmospheric pressure without salt crust formation. The receiver dimensions were chosen to maintain a sufficient temperature to avoid the collapse of the vapor film when the *DNI* is reduced (i.e., to as low as 500 W m<sup>-2</sup>). With the present design, the temperature of the receiver for a *DNI* of 500 W m<sup>-2</sup> is expected to be around 320°C. The construction material, Steel 304L, was chosen based on previously obtained experimental results [20] because of its resistance to high temperatures (having a fusion temperature of 1420°C). The choice of a metallic receiver with high conductivity allows the temperature difference between the upper and lower sides of the receiver to be limited. The mass flow rate in the SB is equal to 699.2 kg h<sup>-1</sup> at 67°C. At the SB outlet, the steam leaves with a flow rate of 454.5 kg h<sup>-1</sup> and the rest of the seawater leaves as brine, both flows being at the equilibrium temperature, i.e., 100.86°C, according to the binary mixture model for seawater used in this study.

Table 3: Design and principal characteristics of the beam-down system and the receiver facility.

Item	Value	Unit
Beam-down system		
Number of heliostats	74	
Reflective area per heliostat	8.5	m <sup>2</sup>
Primary reflective area	629	m <sup>2</sup>
Occupied land	3,350	m <sup>2</sup>
Height of the reflector	20	m
Receiver (specific design calculated for this study)		
Diameter	1.02	m
Thickness	0.08	m
Cone half-angle	15	°
Material	Steel 304L	

### 3.1.3 Integration of the MED part

Concerning the MED part of the system, the temperature and pressure simulation results are presented in Figure 7 for each stage. In addition, Table 4 lists the intermediary mass flows for each of the 14 stages.

It can be seen that the pressure needs to be maintained between 0.290 bars and 0.046 bars for the different stages. This pressure variation permits boiling to occur between 70°C and 32°C; this agrees with data found in the literature [14],[42].

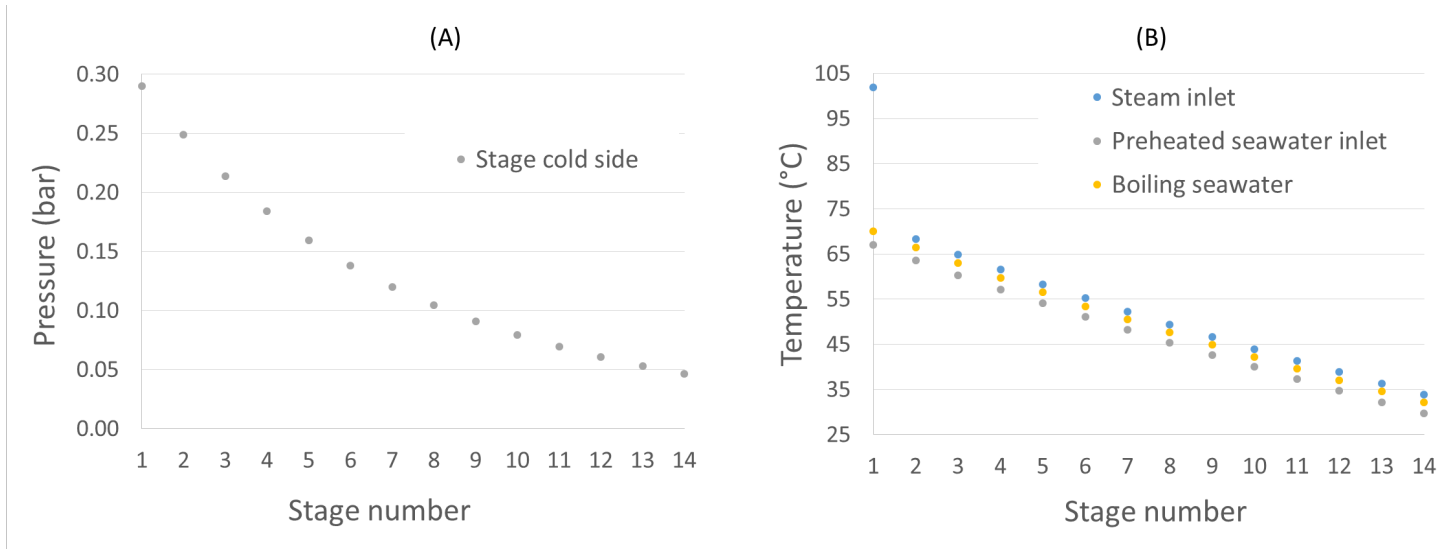


Figure 7: (A) Pressure and (B) temperature levels in the different stages of the MED part of the SB-MED system.

Table 4: Input–output flow rates in the MED part of the SB-MED system.

Stage	Steam inlet [kg h <sup>-1</sup> ]	Extracted vapor flow for preheating [kg h <sup>-1</sup> ]	Seawater inlet [kg h <sup>-1</sup> ]	Steam outlet [kg h <sup>-1</sup> ]
1	454	0	699	438
2	443	8	699	439
3	430	12	699	426
4	415	15	699	411
5	399	18	699	395
6	381	21	699	377
7	361	24	699	358
8	340	27	699	337
9	318	30	699	315
10	295	32	699	291
11	270	35	699	267

12	244	37	699	241
13	217	40	699	214
14	190	42	699	186

### 3.2 Comparison of SB-MED with SB in standalone

Before considering the performance of the SB-MED system and comparing it with conventional desalination technologies, we consider a standalone SB, without recovery of the heat of the steam in an MED. In a standalone SB, all the steam produced is condensed. Part of the condensation energy is used to preheat the input water, and the rest is evacuated with the cooling seawater. Heat and mass flows are presented in Table 5 to allow a comparison between standalone SB and SB-MED.

Table 5: Heat and mass flows in an SB-MED system and an SB-standalone system for comparison.

		Unit	SB-MED system	SB-standalone system
Beam-down	Concentrated power	kW	363.4	3,886.8
SB	Power to water	kW	312.6	3,343.4
	Seawater inlet	kg h <sup>-1</sup>	699	8,158
	Distillate water outlet	kg h <sup>-1</sup>	454	5,303
	Cooling seawater	kg h <sup>-1</sup>	-	550,568
MED	Seawater inlet	kg h <sup>-1</sup>	9,789	-
	Cooling seawater	kg h <sup>-1</sup>	19,492	-
	Distillate water outlet	kg h <sup>-1</sup>	454	-
Total	Distillate water outlet	kg h <sup>-1</sup>	5,303	

It is clear that, for an equivalent flow rate of 5,303 kg h<sup>-1</sup> of distilled water, the required energy transmitted to the water by standalone SB is 10 times higher than that by SB-MED. This implies a 10 times larger solar concentrator installation. The associated material requirements, land occupied, and electrical consumption for the heliostats will therefore be significantly higher. Moreover, in the case of standalone SB, the global flow rate of the seawater required, in the SB and for cooling, is also much larger: 8,158.46 kg h<sup>-1</sup> for standalone SB versus 699.20 kg h<sup>-1</sup> for SB-MED. This significant difference implies greater requirements for pumping and pretreatment. Considering these points, standalone SB is likely not competitive with either conventional technologies or an SB-MED system. Even from an environmental point of view, even though solar energy has a low impact, the enormous differences in the energy performances between standalone SB and SB-MED or conventional technologies will imply a much greater impact in the first case. For this reason, only the SB integrated with a MED system is investigated herein and is further compared with conventional desalination technologies. This integration is fundamental to optimize operating and structural parameters in order to be competitive against conventional desalination technologies.

### 3.3 Energy performance of the SB-MED process

Here, we analyze the three principal components: the solar concentrator, the SB, and the MED.

The optical efficiency of the solar concentrator is defined by the ratio of the concentrated solar energy arriving on the receiver versus the maximal solar energy available at the first reflector. This

efficiency is based on the literature and is fixed at 58.1%. The concentrated solar energy required, 363,414 W, at this optical efficiency implies a large field of heliostats, 629 m<sup>2</sup> for the first reflection mirror. Some improvements can be expected concerning this component that should permit the concentrator size to be reduced at an equivalent productivity.

The SB efficiency can be determined as the ratio of the heat transmitted to the seawater versus the concentrated energy arriving at the receiver. Despite the high temperature of the receiver, the conical shape permits a large part of the radiative losses to be trapped. The chosen design leads to a conversion efficiency of 83.7%, which can be compared with that of conventional boilers (from 95% for a gas boiler to 88%–92% for a coal boiler [43]). Moreover, note that, even if the thermal performance of the SB is slightly smaller, the incoming energy is free and has no environmental impact. In addition, optimization in the design (such as the use of other materials with better characteristics) could increase the overall performance of the SB. The SB is in its early stage of development, significant progress on its performance can be expected in the future. An optimization of its design (including the choice of the material) could bring a significant improvement of the steam production process. Finally, the performance of the MED system should not be defined purely by the energy efficiency because the final product is not energy but desalinated water. The gain output ratio (GOR) is conventionally used to evaluate the performance of such a system and is defined as the ratio of the net distilled flow rate versus the first stage steam flow rate. For the present system, the GOR is equal to 11.7; this value can be compared with the ideal case where the quantity of the generated vapor at each stage is equal to the entering quantity of vapor, in which case the maximal GOR is 14.

To place the SB-MED process within the field of desalination technologies, a first comparison with the conventional processes presented in Section 2.3.1 based on the energy consumption defined by the ratio of the consumed energy versus the quantity of distilled water is proposed. Because thermal and electrical energy cannot be directly compared, the electrical efficiency and thermal consumption of the systems will be presented separately.

The results are presented in Table 6. Note that the results obtained for the conventional desalination scenarios agree with data found in the literature. Indeed, for RO, the usual values of the electricity consumption range from 2 kWh m<sup>-3</sup> to 6 kWh m<sup>-3</sup> [44],[45]. Regarding MED technology, the heat consumption is generally considered to be between 40 kWh m<sup>-3</sup> and 110 kWh m<sup>-3</sup> and the electricity consumption is generally between 1.5 kWh m<sup>-3</sup> and 2.5 kWh m<sup>-3</sup> [18],[46].

Table 6: Heat and electricity consumption of the four compared desalination systems, where RO indicates reverse osmosis and ROR indicates reverse osmosis with energy recovery.

Scenarios	Consumption [kWh m <sup>-3</sup> ]	
	Electricity	Heat
SB-MED	1.39	58.9 (solar)
MED	1.58	58.4 (fossil)
RO	5.37	-
ROR	4.03	-

In terms of heat, the needs of conventional MED are lower than the amount required by the solar approach; however, the results are very close. This conclusion needs to be tempered by the

fundamental difference between the types of energy used: solar, shown in red, versus fossil fuel. Indeed, the efficiency of the SB can be defined by the ratio of heat transmitted to the seawater versus that of the concentrated heat received. This efficiency is equal to 86% and can be compared with the conventional gas boiler efficiency, which is usually close to 95%. Moreover, because of the medium efficiency of the solar field (58%), a large reflector surface is required. However, it is important to emphasize that the environmental and economic cost of the use of solar energy comes only from the construction of the collector and the receiver, unlike the use of fossil energy whose impact and cost are linked to their construction as well as to fuel consumption.

The results presented in Table 6 show the real benefit of the SB-MED solution in terms of electricity consumption. Indeed, even if the SB-MED electricity consumption is slightly higher (13.7%) than that of conventional MED, it is 60.8% lower than that of the ROR scenario, which represents the most-used technology today. The increase in consumption compared with MED can be explained by the heliostat field consumption necessary for solar tracking. Focusing on the electricity in the SB-MED system, the principal consumption points are the following: pumping the seawater from the ocean (42.4%), pretreatment (28.8%), and extraction of the non-condensable gases (17.7%); the rest of the consumption is used for solar tracking and circulation of the water in the SB-MED system.

### 3.4 Environmental performance of the SB-MED system and comparison with conventional desalination technologies

#### 3.4.1. Life cycle inventory results

The inventory results for the four studied systems (the reference SB-MED system and the three conventional desalination systems) are presented in Table 7. The results are expressed with respect to the functional unit, i.e., 1 m<sup>3</sup> of tap water produced. More details concerning the inventory results are given in Appendix 3.

Regarding infrastructure and equipment, the SB-MED process requires more material than the other scenarios; this is primarily due to the oversizing of the MED to compensate for the lower number of annual operating hours and the construction of the heliostats. Indeed, the use of solar energy implies working with higher flow rates for a shorter period to achieve equivalent annual productivity to that of conventional technologies, which operate nearly all year round. In addition, the RO and ROR scenarios require membrane modules for the RO process.

The quantities of seawater pumped for the SB-MED and MED systems are greater than those pumped for the RO and ROR systems, that is, 5.15 m<sup>3</sup> and 5.11 m<sup>3</sup> per 1 m<sup>3</sup> of tap water for the SB-MED and MED processes, respectively, versus 2.33 m<sup>3</sup> per 1 m<sup>3</sup> of tap water for the membrane processes. The additional seawater flow in the SB-MED and MED systems is necessary for the cooling of the final stage of the MED. Similarly, the brine outlets differ in the two situations (brine is rejected to the sea). For the thermal systems, it is possible to mix the brine with the cooling water, which leads to a smaller salinity difference between the brine outlet and the seawater compared with the case in membrane technologies. The discharged effluents for the SB-MED and MED systems also carry heat because their temperatures are higher than the seawater temperature. Salt and heat returning into the sea have no global impact but could have local impacts on restricted areas [47],[48]. Because of the current lack of assessment models, it is not possible to properly quantify these impacts at the moment.

Regarding the end-of-life processes, materials such as concrete or steel were not considered because they can easily be recycled. Only waste destined for disposal, such as membrane modules and cartridge filters, were considered in the landfill disposal. These materials are a mixture of plastic and

polypropylene waste. In addition, the pretreatment step produces sludge, which needs to be further treated. The larger quantity of seawater pretreated in thermal desalination systems implies the production of 2.2 times more sludge than in membrane systems.

Table 7: Inventory and ecoinvent unit processes for the four desalination scenarios.

Category	Material	Input / output	Quantity per m <sup>3</sup> of produced tap water				Unit	ecoinvent process
			SB-MED	MED	RO	ROR		
Equipment and building	Building construction	In	$3.38 \times 10^{-4}$	$2.99 \times 10^{-4}$	$3.18 \times 10^{-4}$	$3.18 \times 10^{-4}$	m <sup>2</sup>	market for building, hall, steel construction [GLO]
	Charcoal for filtration	In	-	-	$1.70 \times 10^{-3}$	$1.70 \times 10^{-3}$	kg	market for charcoal [GLO]
	Concrete	In	$18.60 \times 10^{-5}$	$5.75 \times 10^{-5}$	$3.68 \times 10^{-5}$	$3.68 \times 10^{-5}$	m <sup>3</sup>	unreinforced concrete production, with cement CEM II/B [RoW]
	Land occupation	In	$34.85 \times 10^{-2}$	$1.20 \times 10^{-2}$	$1.27 \times 10^{-2}$	$1.27 \times 10^{-2}$	m <sup>2</sup> year	N/A
	Heliostat mirror	In	$1.69 \times 10^{-2}$	-	-	-	kg	flat glass production, coated [RER]
	Membrane module	In	-	-	$1.25 \times 10^{-3}$	$1.25 \times 10^{-3}$	m <sup>2</sup>	seawater reverse osmosis module production, 8-inch spiral wound, enhanced [GLO]
	Motor	In	$939.75 \times 10^{-6}$	$5.00 \times 10^{-6}$	$5.00 \times 10^{-6}$	$5.00 \times 10^{-6}$	kg	market for electric motor, for electric scooter [GLO]
	Pipe	In	$11.67 \times 10^{-3}$	$7.00 \times 10^{-3}$	$5.37 \times 10^{-3}$	$5.37 \times 10^{-3}$	m	polyethylene pipe production, corrugated, DN 75 [RER]
	Cartridge filter	In	-	-	$1.78 \times 10^{-4}$	$1.78 \times 10^{-4}$	kg	polypropylene production, granulate [RER]
	Pump	In	$2.73 \times 10^{-4}$	$0.68 \times 10^{-4}$	$9.50 \times 10^{-4}$	$9.50 \times 10^{-4}$	unit	market for pump, 40W [GLO]
	Pump station	In	$84.81 \times 10^{-8}$	$18.29 \times 10^{-8}$	$9.02 \times 10^{-8}$	$9.02 \times 10^{-8}$	unit	pump station construction [RoW]
	Sand for filtration	In	-	-	$1.02 \times 10^{-3}$	$1.02 \times 10^{-3}$	kg	market for sand [GLO]
	Steel	In	$1.36 \times 10^{-1}$	$0.04 \times 10^{-1}$	$0.03 \times 10^{-1}$	$0.04 \times 10^{-1}$	kg	hot rolling, steel [RER]
	Stainless Steel	In	$19.64 \times 10^{-3}$	$1.08 \times 10^{-3}$	-	-	kg	steel production, chromium steel 18/8, hot rolled [RER]
Chemical	Carbon dioxide	In	$4.40 \times 10^{-2}$	$4.40 \times 10^{-2}$	$4.40 \times 10^{-2}$	$4.40 \times 10^{-2}$	kg	carbon dioxide production, liquid [RER]
	Scale inhibitors	In	$5.65 \times 10^{-3}$	$5.60 \times 10^{-3}$	$2.55 \times 10^{-3}$	$2.55 \times 10^{-3}$	kg	polycarboxylates production, 40% active substance [RER]
	Citric acid	In	-	-	$5.61 \times 10^{-4}$	$5.61 \times 10^{-4}$	kg	citric acid production [RER]
	Disinfectant	In	$3.57 \times 10^{-3}$	$2.34 \times 10^{-3}$	$2.15 \times 10^{-3}$	$2.15 \times 10^{-3}$	kg	sodium hypochlorite production, product in 15% solution state [RER]
	Hydrogen peroxide	In	-	-	$2.80 \times 10^{-5}$	$2.80 \times 10^{-5}$	kg	hydrogen peroxide production, product in 50% solution state [RER]
	Coagulant	In	$5.65 \times 10^{-2}$	$5.623 \times 10^{-2}$	$2.56 \times 10^{-2}$	$2.56 \times 10^{-2}$	kg	market for iron(III) chloride, without water, in 14% iron solution state [GLO]
	Minerals	In	$1 \times 10^{-1}$	$1 \times 10^{-1}$	$1 \times 10^{-1}$	$1 \times 10^{-1}$	kg	lime production, milled, packed [RoW]
	Dechloration products	In	-	-	$4.62 \times 10^{-4}$	$4.62 \times 10^{-4}$	kg	chlor-alkali electrolysis, mercury cell [RER]
	Water for cleaning	In	-	-	$2.74 \times 10^{-2}$	$2.74 \times 10^{-2}$	kg	tap water production, underground water without treatment [Europe without Switzerland]
Electricity	In	1.58	1.39	5.37	4.03	kWh	market for electricity, low voltage [IT]	
Process	Seawater (inlet)	In	5.15	5.11	2.33	2.33	m <sup>3</sup>	N/A
	Solar energy	In	117.89	-	-	-	kWh	N/A
	Heat	In	-	58.36	-	-	kWh	heat production, natural gas, at boiler modulating <100 kW [Europe without Switzerland]
	Seawater (outlet)	Out	4.15	4.11	1.33	1.33	m <sup>3</sup>	N/A
	Chloride	Out	21.47	21.47	22.32	22.32	kg	N/A
	Sodium ions	Out	11.94	11.94	12.41	12.41	kg	N/A
	Sulfate	Out	3.01	3.01	3.13	3.13	kg	N/A
	Magnesium	Out	1.43	1.43	1.49	1.49	kg	N/A
	Calcium ions	Out	$4.56 \times 10^{-1}$	$4.56 \times 10^{-1}$	$4.74 \times 10^{-1}$	$4.74 \times 10^{-1}$	kg	N/A
	Potassium ions	Out	$4.29 \times 10^{-1}$	$4.29 \times 10^{-1}$	$4.46 \times 10^{-1}$	$4.46 \times 10^{-1}$	kg	N/A
	Hydrogen carbonate	Out	$1.17 \times 10^{-1}$	$1.17 \times 10^{-1}$	$1.22 \times 10^{-1}$	$1.22 \times 10^{-1}$	kg	N/A
	Bromide	Out	$7.41 \times 10^{-2}$	$7.41 \times 10^{-2}$	$7.70 \times 10^{-2}$	$7.70 \times 10^{-2}$	kg	N/A
	Strontium	Out	$7.80 \times 10^{-3}$	$7.80 \times 10^{-3}$	$8.11 \times 10^{-3}$	$8.11 \times 10^{-3}$	kg	N/A
	Boron	Out	$5.07 \times 10^{-3}$	$5.07 \times 10^{-3}$	$5.27 \times 10^{-3}$	$5.27 \times 10^{-3}$	kg	N/A
	Fluoride	Out	$1.56 \times 10^{-3}$	$1.56 \times 10^{-3}$	$1.62 \times 10^{-3}$	$1.62 \times 10^{-3}$	kg	N/A
	Heat waste	Out	41.42	41.42	-	-	kWh	N/A
End of life	Membrane waste	Out	-	-	$1.73 \times 10^{-3}$	$1.73 \times 10^{-3}$	kg	treatment of waste plastic, mixture, sanitary landfill [Europe without Switzerland]
	Sludge	Out	28.26	28.15	12.82	12.82	kg	drying, sewage sludge [RoW]
	Waste from caterbridge	Out	-	-	$1.78 \times 10^{-4}$	$1.78 \times 10^{-4}$	kg	treatment of waste polypropylene, sanitary landfill [RoW]

### 3.4.2. Environmental impact results

The endpoint impact results estimated using the ReCiPe (Endpoint (H,A)) method are presented in Figure 8 for the production of 1 m<sup>3</sup> of tap water by each of the four scenarios.

The total impact of SB-MED is 6.4 times lower than that of conventional MED. Because of the similarities of the MED processes in the two scenarios, the categories “end of life,” “electricity,” and “chemicals” have roughly the same impact in both cases. The impact of “building and infrastructure” is considerably higher in the SB-MED scenario, 3.3 times larger than that in the conventional MED scenario. This difference is explained by the construction of the large solar installation for the SB and because of the oversizing of the MED necessary to compensate for the discontinuity in the solar energy received. However, this is more than compensated for by avoiding the impact associated with burning fossil fuels. Indeed, 88.3% of the impact of conventional MED is caused by the generation of heat from the combustion of natural gas.

The total impact of SB-MED is slightly lower than those of the two RO scenarios. Similar to the above-discussed case, the infrastructure of the SB and the oversizing of the MED installation lead to a 2.6 times higher impact of the SB-MED system than those of the RO systems. The end of life also has a greater impact, 0.09 for SB-MED versus 0.05 for RO. This difference is due to the large quantity of sludge from the water treatment, that is, the water necessary for cooling the final MED stage (as explained in Section 3.3.1). The main advantage of the SB in terms of impact comes from the reduction in the electricity consumption. Indeed, a 0.20 and 0.12 point of impact difference are noted relative to RO and ROR, respectively.

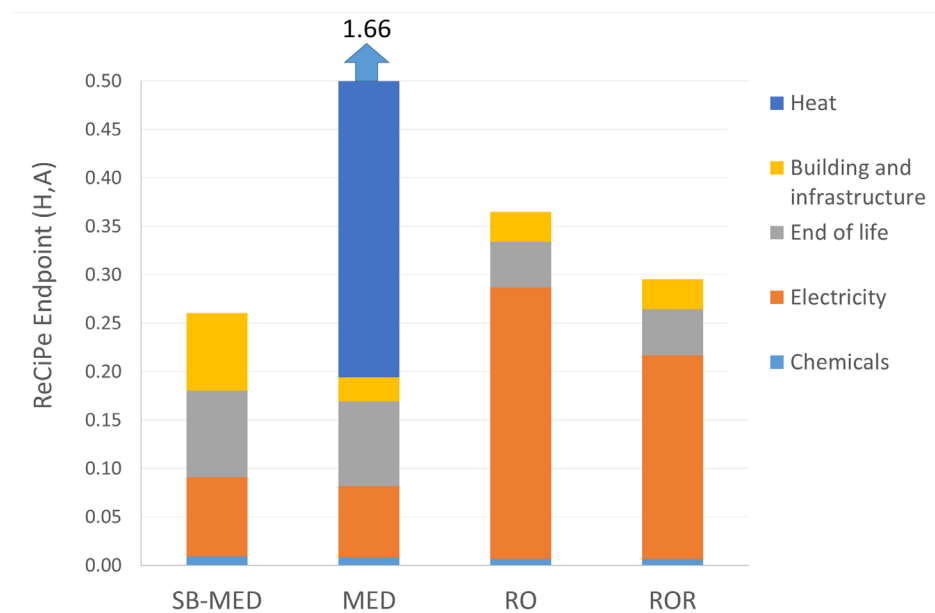


Figure 8: ReCiPe endpoint impact results for the four desalination scenarios.

Figure 9 details the endpoint impact results for the different ReCiPe impact categories. For all scenarios, the greatest impact is related to the use of fossil fuels. Indeed, “climate change, ecosystems,” “climate change, human health,” and “fossil depletion” are linked to the extraction of fossil fuels and the emissions of greenhouse gases during their combustion. This link is direct in the

case of the MED with the gas burner or indirect in all cases with the production of electricity and materials.

Regarding the other impacts, the “urban land occupation” impact of the SB-MED system is greater than those of the other scenarios. This impact is due to the large field of heliostats required for the solar concentration. Note that parallel use of the land under the heliostats field may be possible, for example, for forage or other vegetation growth. This possibility has not been considered in this study but can significantly reduce this impact. The metal required for the equipment also has a large impact on the “metal depletion” category.

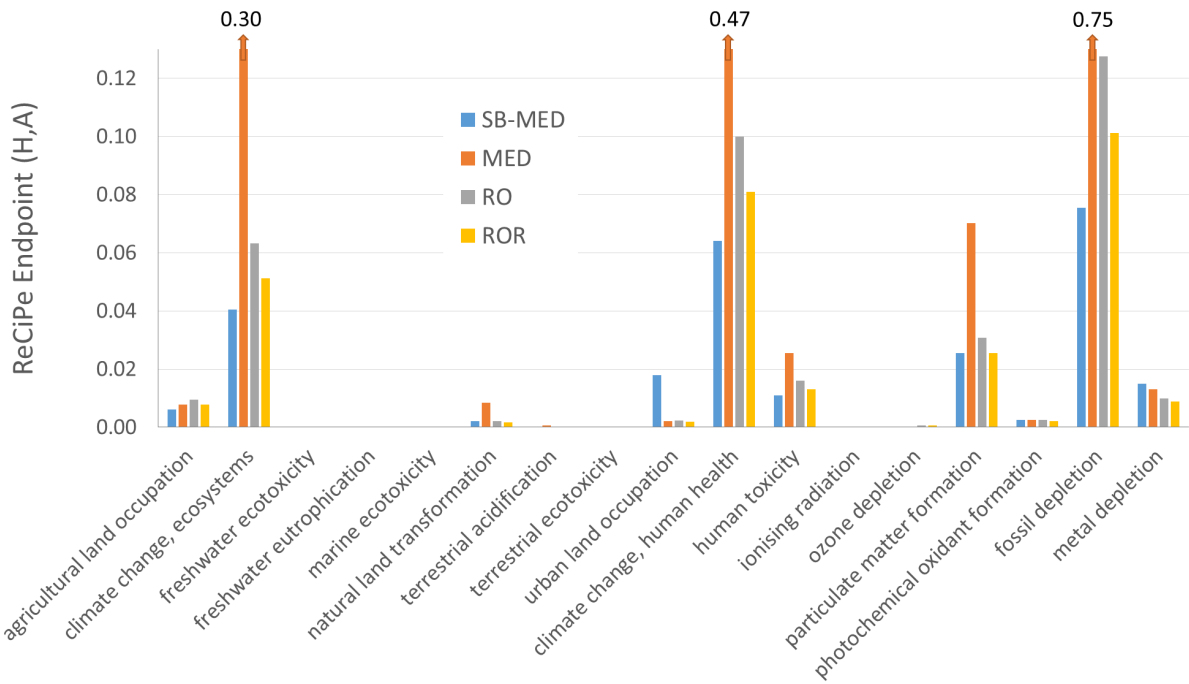


Figure 9: Impact results for SB-MED in comparison with the conventional scenarios.

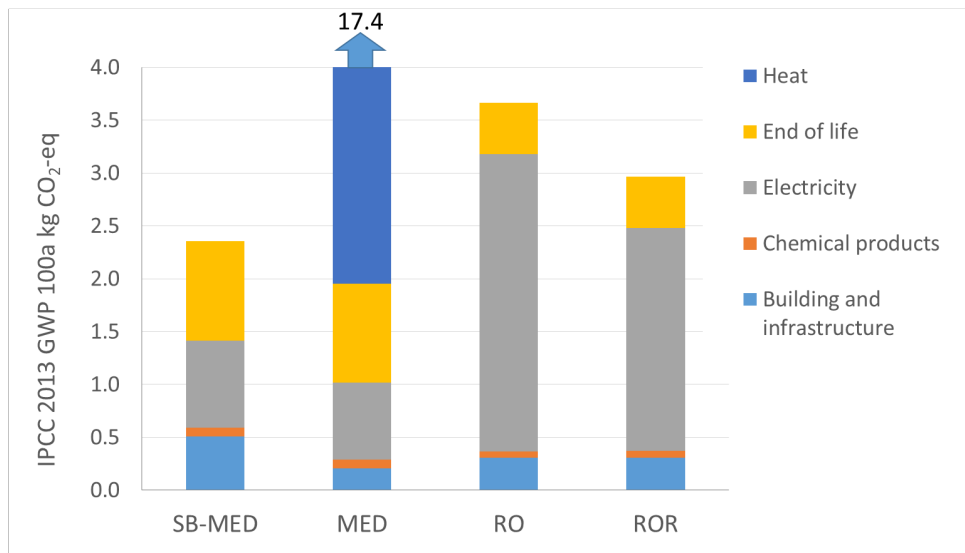


Figure 10: Climate change impact results according to the IPCC2013 (GWP100) method.

Climate change was identified as the main contributor to the ReCiPe endpoint impacts. Figure 10 shows the complementary climate change impact calculated via the IPCC2013 method using GWP100 (the global warming potential at 100 years) and expressed in kg CO<sub>2</sub>-eq. Focusing on this point, the appeal of SB-MED is even greater and the difference between SB-MED and ROR is more significant, with 20.6% kg CO<sub>2</sub>-eq less emissions for the reference case. Regarding the impact contributions of the different processes, the proportions remain roughly the same. The energy contribution to the impact is definitively lower in the case of SB-MED than in the other scenarios.

As observed above, an important aspect to be considered is the electricity mix used: depending on the electricity mix, the ranking of the scenarios could change. As presented in Section 2.3, the calculation was performed with an Italian electricity mix used as the reference. Electricity is one of the most important sources of impact, especially for the RO scenarios. Accordingly, the use of an electricity mix that emits more CO<sub>2</sub>, which is the case in many countries using desalination (e.g., Kuwait, Saudi Arabia, or Australia) [26], will degrade the environmental performance of the system. Moreover, in case of SB-MED, the location will have important consequences on the share of impacts between the infrastructure and the functioning. Indeed, with better solar power, given the same installation, the tap water productivity will be greater. Figure 11 shows the climate change impact calculated with IPCC2013 using three different electricity mixes: the reference (e.g., Italy), a low-carbon mix (e.g., France), and a high-carbon mix (e.g., Australia). Because SB-MED consumes less electricity, the impact of the electrical mix is less important for SB-MED. Switching from an Italian mix to an Australian mix increases the CO<sub>2</sub>-equivalent emission by 35.2%, while using a French mix decreases it by 26.9%. The same modification increases the emission for the ROR scenario by 71.4% for the Australian mix and decreases it by 54.7% for the French mix. In addition, it appears that, in the case of a low-carbon electricity mix, the ROR solution becomes even more advantageous in terms of its climate impact than the SB-MED solution.

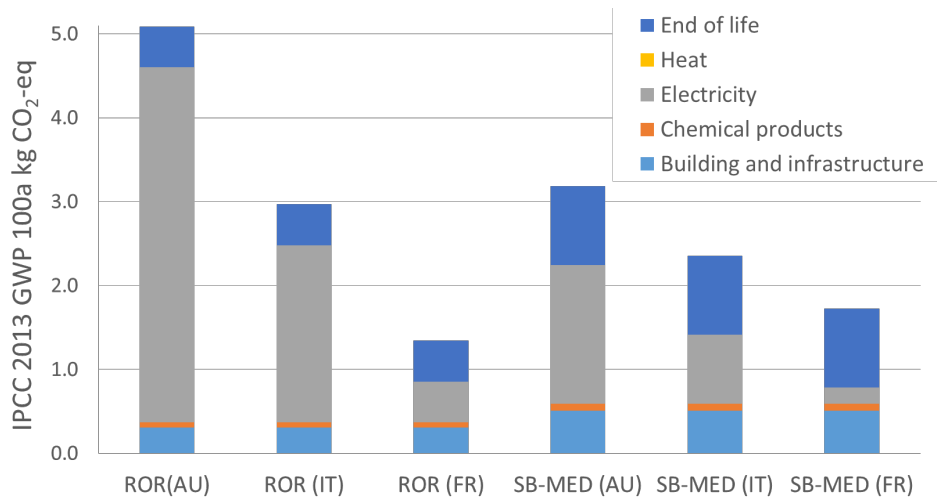


Figure 11: Climate change impact results for SB-MED and ROR for the Corsican (Italian, IT), French (FR) and Australian (AU) electricity mixes.

This analysis of the electricity-mix impact considers only the climate change impact; other considerations (e.g., other environmental impacts and technological risks) are beyond the scope of this analysis.

Note that the SB-MED system is a new concept and complementary work needs to be done to prove its feasibility at the industrial level. Despite there being much room for improvement in this technology, the current results indicate that this process could be environmentally competitive with the currently most-advanced RO desalination process.

Regarding the main aspects that need to be investigated, the design of the collector system could be improved. Construction has a significant impact, and improving the performance of the solar collector or reducing the material consumption for an identical technical performance could greatly improve the environmental performance of the system. Furthermore, the scale-up of the SB needs to be investigated at larger scales and the scale effect on the overall performance needs to be evaluated.

Concerning the design of the MED part, the chosen configuration with 14 stages enables a performance that is representative of what could be observed at an industrial scale but is not necessarily the best performance that can be obtained. Different design improvements (such as increasing the number of stages) may lead to an increase in the productivity of the system.

The substantial difference in the environmental impact between conventional MED and SB-MED suggests that the addition of an SB to an already existing MED installation is a mitigation solution worth exploring. Indeed, many countries that use desalination have available land and a strong solar potential. In this context, SBs could be very effective and relatively easy to connect to already existing thermal desalination facilities. Considering the significant impact of burning fossil fuels in a conventional MED facility (15.43 kg CO<sub>2</sub>-eq per m<sup>3</sup> of tap water in the considered example), replacing at least part of this energy source with concentrated solar energy could save enough emissions to offset the impact of the construction of the solar installation (approximately 0.51 kg CO<sub>2</sub>-eq per m<sup>3</sup> of tap water in the considered example). This could, in time and with reasonable investment, significantly reduce the fuel consumption and associated impact of thermal desalination plants already in operation.

## Conclusions

In this study, an innovative process coupling a beam-down concentrator with a solar boiler and multiple-effect distillation (SB-MED) was proposed, allowing an alternative approach in the field of water desalination. A theoretical model was developed to describe this new process “from sea and sun to tap water”. Applied to a reference case, the model allowed to investigate the feasibility of tap water production for a small community, i.e., an annual production of 10,000 m<sup>3</sup>. The facility was sized in terms of equipment, materials, and energy consumption.

The energy consumption of this process was estimated to be 1.58 kWh of electricity and 117.7 kWh of direct solar energy per 1 m<sup>3</sup> of tap water produced. An area of 3,485 m<sup>2</sup> is needed to supply the target annual production, this area primarily being occupied by the concentrating solar facility.

The appeal of coupling SB and MED was demonstrated. Indeed, if the SB uses low-impact solar energy resources, its standalone use suffers from a lack of efficiency compared with the SB-MED system. The required energy for boiling in a standalone SB system is 10 times higher than that in an SB-MED system. This implies a 10 times larger solar concentrator installation in the case of standalone SB. The SB-MED system is therefore particularly competitive in terms of both energy performance and environmental impact. The energy reuse strategy enabled by this solution gives results equivalent to the best RO technologies in the field. These results were obtained for the reference case, and further optimizations could improve them.

A significant part of the impact in the proposed solution is caused by the construction of the equipment. The integration of heat storage could be beneficial in terms of the environmental performance by allowing more stable operation and a reduction in the dimensions of the MED, pretreatment, and post-treatment installations, with an associated reduction in their impacts.

This comparison of the SB-MED system with conventional desalination technologies demonstrated that, at equivalent productivity, the SB-MED system requires less electricity than the best-case RO scenario. Compared with conventional MED, a reasonable increase in the electricity consumption permits the use of fossil fuels to be avoided. In addition, considering the low level of modifications to the MED part of the SB-MED system compared with conventional MED, consideration should be given to installing SBs as plug-in modules in already operational MEDs. This addition could significantly reduce the impacts of existing desalination plants. The overall endpoint impact of SB-MED, estimated via the ReCiPe method, was significantly lower than that of MED and was in the range of those of the RO processes. The same trend was observed for the climate change impact. The presented results emphasize the potential interest of this new process, which could be an alternative solution to RO when solar energy is abundant and the electricity mix is highly CO<sub>2</sub> emitting.

In perspective, pilot experiments and optimization of the process design are needed together with an iterative, environmental and economic assessment, including the regional specificities in terms of solar energy availability and energy storage.

## Acknowledgments

This research was funded by INSA (Institut National des Sciences Appliquées) Toulouse, and CNRS (Centre National de la Recherche Scientifique), France. We thank Martha Evonuk, PhD, from Evonuk Scientific Editing (<http://evonukscientificediting.com>) for editing a draft of this manuscript.

## References

- [1] S. Uhlenbrook, The United Nations world water development report 2019: leaving no one behind. United Nations Educational, Scientific and Cultural Organization, 2019.
- [2] H. Zhao, S. Qu, S. Guo, H. Zhao, S. Liang, et M. Xu, « Virtual water scarcity risk to global trade under climate change », *Journal of Cleaner Production*, vol. 230, p. 1013-1026, sept. 2019, doi: 10.1016/j.jclepro.2019.05.114.
- [3] M. M. Mekonnen et A. Y. Hoekstra, « Four billion people facing severe water scarcity », *Science Advances*, vol. 2, no 2, p. e1500323, févr. 2016, doi: 10.1126/sciadv.1500323.
- [4] N. G. D. Center, « Volumes of the World's Oceans from ETOPO1 ». [https://ngdc.noaa.gov/mgg/global/etopo1\\_ocean\\_volumes.html](https://ngdc.noaa.gov/mgg/global/etopo1_ocean_volumes.html) (consulté le juin 21, 2021).
- [5] M. A. Darwish, F. M. Al-Awadhi, et A. M. Darwish, « Energy and water in Kuwait Part I. A sustainability view point », *Desalination*, juin 2007, Consulté le: mars 20, 2019. [En ligne]. Disponible sur: <https://www.sciencedirect.com/science/article/pii/S0011916408001136>
- [6] V. K. Chauhan, S. K. Shukla, J. V. Tirkey, et P. K. Singh Rathore, « A comprehensive review of direct solar desalination techniques and its advancements », *Journal of Cleaner Production*, vol. 284, p. 124719, févr. 2021, doi: 10.1016/j.jclepro.2020.124719.
- [7] J. Kucera, *Reverse Osmosis: Industrial Processes and Applications*, 2nd Edition, 2e éd. Wiley, 2015. Consulté le: mai 02, 2019. [En ligne]. Disponible sur: <https://www.wiley.com/en-as/Reverse+Osmosis%3A+Industrial+Processes+and+Applications%2C+2nd+Edition-p-9781118639740>
- [8] H. Chua et B. Rahimi, *Low Grade Heat Driven Multi-Effect Distillation and Desalination*. 2017.
- [9] M. Mannan, T. Al-Ansari, H. R. Mackey, et S. G. Al-Ghamdi, « Quantifying the energy, water and food nexus: A review of the latest developments based on life-cycle assessment », *Journal of Cleaner Production*, vol. 193, p. 300-314, août 2018, doi: 10.1016/j.jclepro.2018.05.050.
- [10] K. Elsaid, M. Kamil, E. T. Sayed, M. A. Abdelkareem, T. Wilberforce, et A. Olabi, « Environmental impact of desalination technologies: A review », *Science of The Total Environment*, vol. 748, p. 141528, déc. 2020, doi: 10.1016/j.scitotenv.2020.141528.
- [11] C. Koroneos, A. Dompros, et G. Roumbas, « Renewable energy driven desalination systems modelling », *Journal of Cleaner Production*, vol. 15, no 5, p. 449-464, janv. 2007, doi: 10.1016/j.jclepro.2005.07.017.
- [12] J. Bundschuh, M. Kaczmarczyk, N. Ghaffour, et B. Tomaszewska, « State-of-the-art of renewable energy sources used in water desalination: Present and future prospects », *Desalination*, vol. 508, p. 115035, juill. 2021, doi: 10.1016/j.desal.2021.115035.
- [13] V. G. Gude, N. Nirmalakhandan, et S. Deng, « Renewable and sustainable approaches for desalination », *Renewable and Sustainable Energy Reviews*, vol. 14, no 9, p. 2641-2654, déc. 2010, doi: 10.1016/j.rser.2010.06.008.
- [14] P. Palenzuela, D.-C. Alarcón-Padilla, et G. Zaragoza, *Concentrating Solar Power and Desalination Plants: Engineering and Economics of Coupling Multi-Effect Distillation and Solar Plants*. Springer International Publishing, 2015. Consulté le: mars 28, 2019. [En ligne]. Disponible sur: <https://www.springer.com/la/book/9783319205342>

- [15] J. F. Servert, E. Cerrajero, et E. L. Fuentealba, « Synergies of solar energy use in the desalination of seawater: A case study in northern Chile », AIP Conference Proceedings, vol. 1734, no 1, p. 140002, mai 2016, doi: 10.1063/1.4949232.
- [16] W. He, Y. Wang, et M. H. Shaheed, « Stand-alone seawater RO (reverse osmosis) desalination powered by PV (photovoltaic) and PRO (pressure retarded osmosis) », juin 2015, doi: 10.1016/j.energy.2015.04.046.
- [17] T. Espino, B. Peñate, G. Piernavieja, D. Herold, et A. Neskakis, « Optimised desalination of seawater by a PV powered reverse osmosis plant for a decentralised coastal water supply », Desalination, vol. 156, no 1, p. 349-350, août 2003, doi: 10.1016/S0011-9164(03)00365-5.
- [18] F. Trieb et al., « Aqua-CSP Concentrating Solar Power for Seawater Desalination », nov. 2007.
- [19] J. Wellmann, B. Meyer-Kahlen, et T. Morosuk, « Exergoeconomic evaluation of a CSP plant in combination with a desalination unit », Renewable Energy, vol. 128, no PB, p. 586-602, 2018.
- [20]
- [21] Marwan Mokhtar, S. A. Meyers, P. R. Armstrong, et M. Chiesa, « Performance of a 100 kWth Concentrated Solar Beam-Down Optical Experiment », J. Sol. Energy Eng, vol. 136, no 4, p. 041007-041007-8, mai 2014, doi: 10.1115/1.4027576.
- [22] M. Diago, N. Calvet, et P. R. Armstrong, « Net power maximization from a faceted beam-down solar concentrator », Solar Energy, vol. 204, p. 476-488, juill. 2020, doi: 10.1016/j.solener.2020.04.061.
- [23] « ISO 14040:2006 - Environmental management - Life cycle assessment - Principles and framework », International Organization for Standardization, sept. 2020.
- [24] A. Maurel, Dessalement de l'eau de mer et des eaux saumâtres : Et autres procédés non conventionnels d'approvisionnement en eau douce, 2e édition. Paris: Tec & Doc Lavoisier, 2006.
- [25] iPoint-systems gmbh, umberto. 2021.
- [26] « ecoinvent ». <https://www.ecoinvent.org/> (consulté le mai 06, 2021).
- [27] N. A. and S. A. NASA, Configuration Factors for Exchange of Radiant Energy Between Axisymmetrical Sections of Cylinders, Cones, and Hemispheres and Their Bases.
- [28] K. E. N'Tsoukpoe et al., « Integrated design and construction of a micro-central tower power plant », Energy for Sustainable Development, vol. 31, p. 1-13, avr. 2016, doi: 10.1016/j.esd.2015.11.004.
- [29] M. F. Modest, Radiative Heat Transfer. Academic Press, 2013.
- [30] WARREN M. Rohsenow, J. P. Hartnett, et Cho Young, Handbook of Heat transfer, 3e éd. 1998. Consulté le: juill. 12, 2019. [En ligne]. Disponible sur: [http://93.174.95.29/\\_ads/E2CC3EEF4382C3824AEC65F3515129CD](http://93.174.95.29/_ads/E2CC3EEF4382C3824AEC65F3515129CD)
- [31] I. H. Bell, J. Wronski, S. Quoilin, et V. Lemort, « Pure and Pseudo-pure Fluid Thermophysical Property Evaluation and the Open-Source Thermophysical Property Library CoolProp », Ind. Eng. Chem. Res., vol. 53, no 6, p. 2498-2508, févr. 2014, doi: 10.1021/ie4033999.
- [32] A. D. Khawaji, I. K. Kutubkhanah, et J.-M. Wie, « Advances in seawater desalination technologies », Desalination, vol. 221, no 1, p. 47-69, mars 2008, doi: 10.1016/j.desal.2007.01.067.

- [33] M. Monnot, G. D. M. Carvajal, S. Laborie, C. Cabassud, et R. Lebrun, « Integrated approach in eco-design strategy for small RO desalination plants powered by photovoltaic energy », *Desalination*, vol. 435, p. 246-258, juin 2018, doi: 10.1016/j.desal.2017.05.015.
- [34] « Lalonde Systhermique - Gaz Incondensables ». <https://www.systhermique.com/fr/gazincondensables.html> (consulté le juill. 28, 2021).
- [35] Mémento des pertes de charges - I.E. Idel'cik - 3ème édition - Librairie Eyrolles. Consulté le: mai 06, 2021. [En ligne]. Disponible sur: <https://www.eyrolles.com/BTP/Livre/memento-des-pertes-de-charges-9782212059007/>
- [36] D. Gille, « Seawater intakes for desalination plants », *Desalination*, vol. 156, no 1, p. 249-256, août 2003, doi: 10.1016/S0011-9164(03)00347-3.
- [37] « CSM ». <http://www.csmfilter.com/> (consulté le mai 26, 2021).
- [38] N. Voutchkov, *Desalination Engineering: Planning and Design*. New York: McGraw-Hill Professional, 2013.
- [39] T. Kodama et al., « Flux Measurement of a New Beam-down Solar Concentrating System in Miyazaki for Demonstration of Thermochemical Water Splitting Reactors - ScienceDirect », *ENERGY PROCEDIA*, vol. 49, 2014, Consulté le: mars 20, 2019. [En ligne]. Disponible sur: <https://www.sciencedirect.com/science/article/pii/S1876610214006651>
- [40] BCP, « BCP solar technology », juill. 02, 2021. [http://www.xinchen-csp.com/en/about.php?class\\_id=101](http://www.xinchen-csp.com/en/about.php?class_id=101) (consulté le juill. 01, 2021).
- [41] Magaldi Group, « Industrila Solar beam down », juill. 02, 2021. <https://www.magaldi.com/en/expertise/solar-energy> (consulté le juill. 01, 2021).
- [42] P. Talebbeydokhti, A. Cinocca, R. Cipollone, et B. Morico, « Analysis and optimization of LT-MED system powered by an innovative CSP plant », *Desalination*, vol. 413, p. 223-233, juill. 2017, doi: 10.1016/j.desal.2017.03.019.
- [43] Esa Kari Vakkilainen, *Steam Generation from Biomass*, 1er edition. Butterworth-Heinemann, 2016. Consulté le: févr. 01, 2021. [En ligne]. Disponible sur: <https://www.sciencedirect.com/book/9780128043899/steam-generation-from-biomass>
- [44] R. G. Raluy, L. Serra, et J. Uche, « Life cycle assessment of desalination technologies integrated with renewable energies », *Desalination*, vol. 183, no 1, p. 81-93, nov. 2005, doi: 10.1016/j.desal.2005.04.023.
- [45] M. Qasim, M. Badrelzaman, N. N. Darwish, N. A. Darwish, et N. Hilal, « Reverse osmosis desalination: A state-of-the-art review », *Desalination*, vol. 459, p. 59-104, juin 2019, doi: 10.1016/j.desal.2019.02.008.
- [46] A. Al-Karaghoul et L. L. Kazmerski, « Energy consumption and water production cost of conventional and renewable-energy-powered desalination processes », *Renewable and Sustainable Energy Reviews*, vol. 24, p. 343-356, août 2013, doi: 10.1016/j.rser.2012.12.064.
- [47] K. L. Petersen et al., « Impact of brine and antiscalants on reef-building corals in the Gulf of Aqaba – Potential effects from desalination plants », *Water Research*, vol. 144, p. 183-191, nov. 2018, doi: 10.1016/j.watres.2018.07.009.

- [48] E. Jones, M. Qadir, M. T. H. van Vliet, V. Smakhtin, et S. Kang, « The state of desalination and brine production: A global outlook - ScienceDirect », *Science of the total environment*, vol. 657, déc. 2018, Consulté le: mars 20, 2019. [En ligne]. Disponible sur: <https://www.sciencedirect.com/science/article/pii/S0048969718349167>
- [49] M. B. Mokhtar, « The Beam-Down Solar Thermal Concentrator: Experimental Characterization and Modeling », Masdar Institute of Science and Technology, Masdar, 2011.
- [50] J. K. Edzwald et J. Haarhoff, « Seawater pretreatment for reverse osmosis: Chemistry, contaminants, and coagulation », *Water Research*, vol. 45, no 17, p. 5428-5440, nov. 2011, doi: 10.1016/j.watres.2011.08.014.
- [51] N. Voutchkov, *Desalination Project Cost Estimating and Management*, 1re éd. Boca Raton: CRC Press, 2018.
- [52] N. Voutchkov, « Considerations for selection of seawater filtration pretreatment system », *Desalination*, vol. 261, no 3, p. 354-364, oct. 2010, doi: 10.1016/j.desal.2010.07.002.
- [53] J. Kavitha, M. Rajalakshmi, A. R. Phani, et M. Padaki, « Pretreatment processes for seawater reverse osmosis desalination systems—A review », *Journal of Water Process Engineering*, vol. 32, p. 100926, déc. 2019, doi: 10.1016/j.jwpe.2019.100926.
- [54] « Powerpal MHG-T1 1kW Hydro Turbine », Renugen. <https://www.renugen.co.uk/powerpal-mhg-t1-1kw-hydro-turbine/> (consulté le mai 26, 2021).